Available online at www.sciencedirect.com

ScienceDirect

Procedia CIRP 104 (2021) 571–575

www.elsevier.com/locate/procedia

54th CIRP Conference on Manufacturing Systems

Tool deflection compensation by drive signal-based force reconstruction and process control

Berend Denkena[a], Benjamin Bergmann[a], Dennis Stoppel[a,*]

[a]*Institute of Production Engineering and Machine Tools, An der Universität 2, 30823 Garbsen, Germany*

* Corresponding author. Tel.: +49-511-762-18327; fax +49-511-762-5115. *E-mail address:* stoppel@ifw.uni-hannover.de

Abstract

Tool deflection is a major cause for shape deviations in milling. Therefore, an approach is presented to compensate tool deflection based on the drive signals of a milling center. First, a real-time capable model is implemented to reconstruct static process forces by using the drive signals of a machine tool. To calculate the actual deflection, the forces are combined with a stiffness model of the tool. Finally, a controller is designed to minimize shape deviation of the workpiece. Based on experimental milling investigations it is shown that tool deflection can be significantly reduced.

Keywords: Process control; milling; drive; machine tool; compensation

1. Introduction

To achieve a robust and efficient production, it is essential to increase the level of autonomy. This also applies to the milling process. One major trend that has to be considered in this context is the increasing variety of machined parts due to product individualization. Consequently, small-batch production increases, while product demand remains the same [1]. Therefore, it is important to avoid rejects when setting up a process to preserve economic efficiency. At the same time, quality limits have to be maintained. Therefore, static and dynamic process errors are to be prevented. Especially tool deflection leads to shape deviations of the workpiece and causes rejections. A detailed analysis of the resulting surface error is provided by Desai and Rao [DES]. In general, factors such as process forces, cantilever length, and tool diameter have a strong impact on the deflection. Nghiep et al. investigated the influence of different process parameters [NG]. They found a strong correlation between width of cut and tool deflection.

While deflection is inevitable, various methods have been researched to compensate for the resulting surface error. The methods can be divided in offline and online approaches. Offline approaches are based on a tool path adaption during process planning. Therefore, Rao and Rao calculated the process forces and the resulting tool deflection. Subsequently, the optimal tool path is determined iteratively [4]. As a result of this approach, the surface error is reduced by 65-78%. Dépincé and Hascoët [5, 6] predict the deflection error based on process parameters of a milling process. In a second step, the tool path is adapted according to the mirror method along the initial path. Soori et al. used a genetic algorithm to find the optimal tool path [7]. Thereby, Soori et al. achieved a reduction of 23.6 % of the deflection error. However, the disadvantage of these offline approaches is that they are only based on simulation. As a consequence, it is not possible to react to time-variant changes like the effect of tool wear.

To overcome this limitation, a process parallel parameter adaption is necessary. Based on the spindle current, Kim et al. developed a feed override control, to reduce the deflection [8].

10.1016/j.procir.2021.11.096

Denkena et al. realized an online compensation that either adapts the feed override [9] or the positional axis offset in feed normal direction [10]. Therefore, the process forces are measured by a sensory spindle slide that is equipped with strain gauges. Depending on the machine tool, up to 83% of the shape deviation were compensated. In case of the override adaption, process time increased by 50%. Another position controller is introduced by Brecher et al. [11], relying on force measurements with a dynamometer. The proactive control approach reduces shape deviation by up to 95%. Furthermore, it is possible to adjust the tool path without inferring with the NC controller. In [12] an adaptronic spindle is developed and used to compensate for the tool deflection. The resulting surface error could be reduced by 60 to 90%. Using a mechatronic tool holder, Yang and Cho tilted the tool to reduce the final shape deviation [13]. It is also possible to combine online and offline approaches, as described in [14]. The above demonstrates that online adaption is capable to reduce shape deviation significantly. However, all cited approaches rely on force measurements. For this purpose, external sensors are used, which have various disadvantages like susceptibility to failure or they introduce restrictions to the workspace. Therefore, this paper presents a new approach for process parallel compensation of tool deflection based on the drive signals of a five-axis milling center. First, section 2 introduces a method to estimate the tool deflection during the milling process. For this purpose, the process forces are reconstructed from the drive current [15] and the bending stiffness of the tool is determined. Subsequently, the controller is introduced in section 3 and results are compared to the compensation based on the sensory spindle slide [9, 10], which can easily be retrofitted on existing machine tools.

Nomenclature

x, y, z	axis coordinates
x_{mcs}	x-axis position in machine coordinates
x_{tcp}	x-axis position of the tool center point
v_x	x-axis velocity
F_x	process force in x-direction
k_m	motor constant of the linear drive of the HSC30
i	motor current
k	spring constant of the restoring force
x_r	virtual resting point regarding restoring forces
m_x	mass of the axis slide
F_{co}	cogging force
F_{fr}	friction force
φ_i	tool orientation
σ	shape deviation
k_p	proportional gain
a_p	depth of cut
E	Young's modulus
I	Inertia

2. Tool deflection estimation

A main component of the tool deflection control is the online estimation of the deflection error. For this reason, the drive signals are evaluated to reconstruct process forces. Also, the tool stiffness is determined with a separate cycle. Using a bending beam model, the deflection error is computed from the reconstructed process forces and the bending stiffness.

2.1. Experimental Setup

The system is implemented on the DMG Mori five-axis milling center HSC30 linear. The spindle moves along x-, y- and z-axis actuated by linear direct drives. Moreover, the machine table is actuated by two rotary actuators (B- and C-Axis). The HSC30 is equipped with a Siemens Sinumerik 840 D solution line control. In addition, the control is connected to a real-time capable Beckhoff industrial PC (IPC) via Process Field Bus (Profibus). The data acquisition and all calculations, including the force model, the deflection estimation, and the process control itself, were performed on the IPC. The drive signals were transmitted in the interpolation cycle of the machine control with a frequency of 250 Hz. All cutting investigations are conducted with end mills mounted in a shrink chuck. The machined material was AISI 1045. To validate the force reconstruction, a Kistler dynamometer 9257 B was used. The signals of the dynamometer were filtered (300 Hz), amplified, and converted (1,000 Hz, 16 Bit).

2.2. Reconstruction of process forces

For force reconstruction, a process force model is used that calculates a 3-dimensional force vector from the signals of the x-, y-, and x-axis drives. The model-based approach is already researched in a previous publication [15]. In summary, the model consists of four sub-models, representing motor cogging forces, linear restoring forces, friction forces, and inertia. Subtracting these forces from the product of motor current and motor constant yields the process force vector, Eq. 1. Transmission losses are omitted since the axis are actuated by linear direct-drive motors without a gear. A major advantage of the model is that it can be parametrized automatically without additional measuring equipment.

$$\begin{bmatrix} F_x \\ F_y \\ F_z \end{bmatrix} = \begin{bmatrix} k_{m,x} & 0 & 0 \\ 0 & k_{m,y} & 0 \\ 0 & 0 & k_{m,z} \end{bmatrix} \begin{bmatrix} i_x \\ i_y \\ i_z \end{bmatrix} - \begin{bmatrix} k_x & 0 & 0 \\ 0 & k_y & 0 \\ 0 & 0 & k_z \end{bmatrix} \begin{bmatrix} x - x_r \\ y - y_r \\ z - z_r \end{bmatrix} - F_{co}(x, y, z) - F_{fr}(\dot{x}, \dot{y}, \dot{z}) - \begin{bmatrix} m_x + m_z & 0 & 0 \\ 0 & m_x + m_y + m_z & 0 \\ 0 & 0 & m_z \end{bmatrix} \begin{bmatrix} \ddot{x} \\ \ddot{y} \\ \ddot{z} \end{bmatrix} \quad (1)$$

The model results indicate that axis movements with a constant feed velocity are reconstructed sufficiently. In Fig. 1 the reconstructed forces are shown in comparison to the measured forces. Comparing the model output to the measurements of a dynamometer, a root mean squared errors (RMSE) of roughly 30 N to 40 N is achieved. A detailed description and evaluation of the used method can be found in [9].

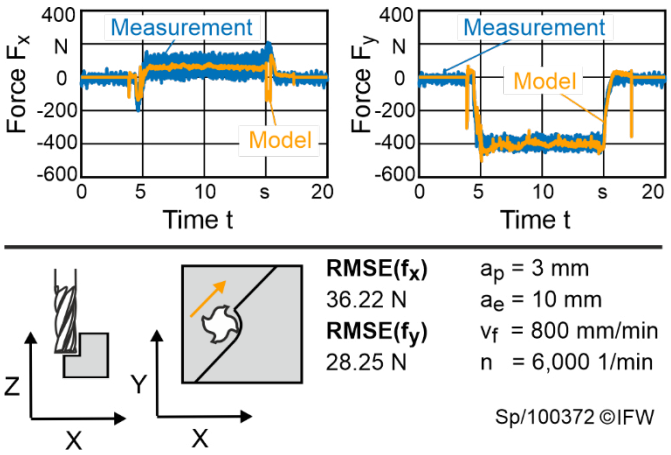

Fig. 1. Reconstructed forces in comparison to measured forces

2.3. Soft collision

To calculate the tool deflection from the reconstructed forces, the bending stiffness of each tool must be estimated. Since the tool-specific area of inertia is generally unknown, a soft collision is carried out to determine the bending stiffness as a product of Young's modulus E and the area of inertia [9]. To perform a soft collision, the tool slowly collides with the workpiece, while collision forces are measured. Compared to [9] there is no external force measurement, but collision forces are estimated by the drive current. The workpiece is prepared to apply a 90° angle between the outer surface and the top, yielding a defined contact surface. To exclude dependence on the tool orientation, the soft collision is executed for evenly distributed rotary angles of the spindle. The whole procedure is illustrated in Fig. 2.

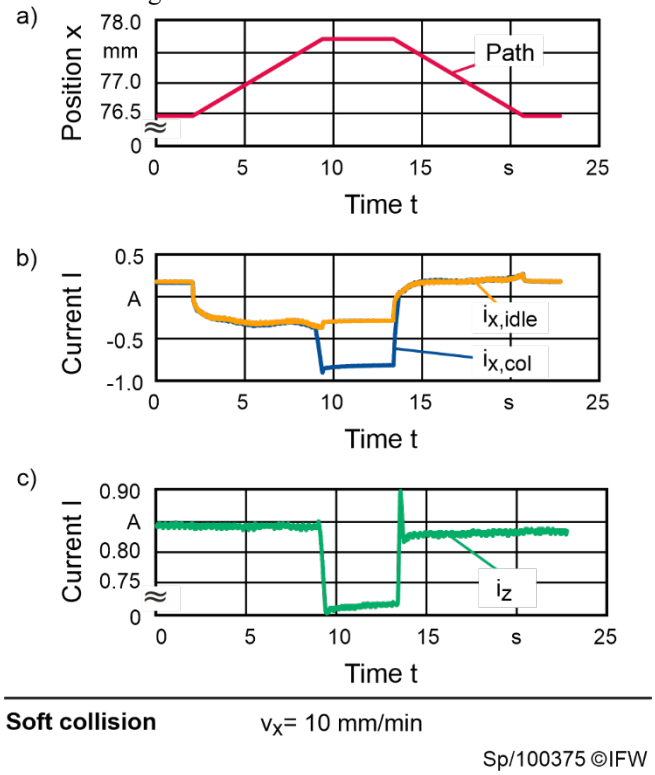

Fig. 2. a) different tool orientations b) soft collision c) axis movement and forces

First the tool center point (x_{tcp}) is located in a defined fallback collision (t_1). Next, the tool is moved in the direction of the workpiece with a constant feed velocity of v_x =10 mm/min (t_2). Due to the workpiece geometry the exact coordinate where the first contact between tool and workpiece happens is generally unknown (t_c). For this reason, the tool stops moving at a predefined coordinate (t_3). After a resting period of 4 seconds, the tool moves back to the fallback position t_1 with a velocity of $-v_x$.

To evaluate the measurements, t_c has to be determined. Therefore, the motor current of the z-axis drive i_z is analyzed. Due to the collision force component in Z-direction, i_z first has a maximum when contact between tool and workpiece happens (t_c), Fig. 3 c). A second maximum which is more prominent occurs when the contact dissolves. The collision distance results from the difference between $x_{tcp}(t_c) = x_{mcs}(t_c) \cong x_{tcp}(t_3)$ and the resting position in machine coordinates $x_{mcs}(t_3)$. Furthermore, the collision force in x-direction can be estimated from the x-axis motor current i_x. Fig. 3 b) shows the motor current during the collision $i_{x,col}$ compared to the current $i_{x,idle}$ during the same axis movement but with the workpiece removed. The difference between both reflects the collision force. Based on the results above, the bending stiffness is calculated with the bending beam equation for each tool orientation [9]. By averaging over all trials, the final bending stiffness is approximated.

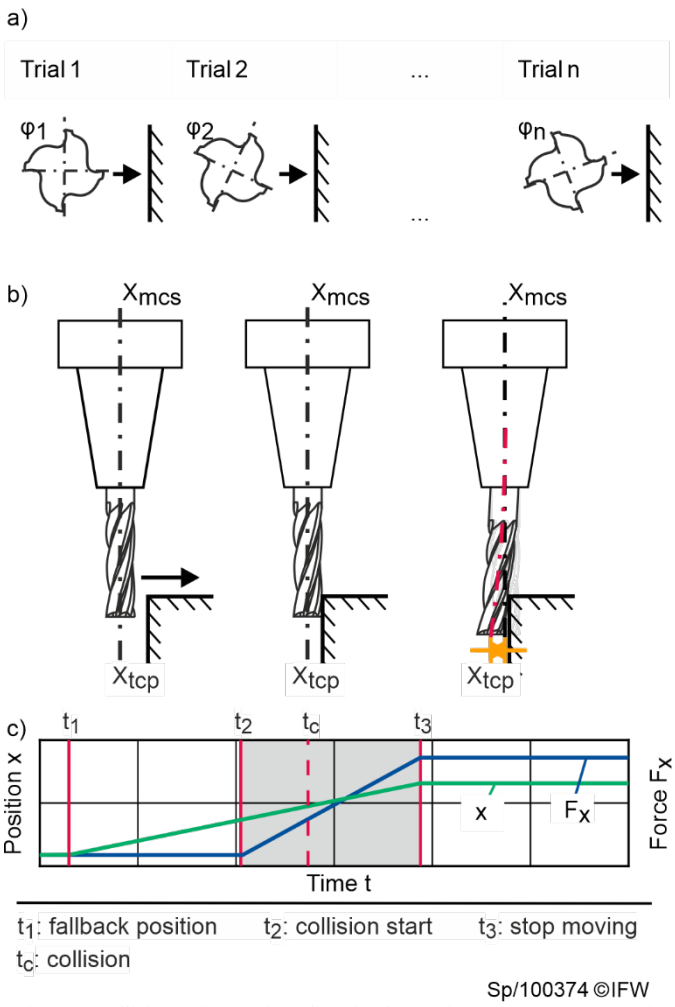

Fig. 3. a) collision trajectory in x-direction b) x-axis motor current c) z-axis motor current

The results of the collision are shown in Fig 4. The calculated stiffness varies between 18 Nm² and 40 Nm². These results indicate that there is a significant dependency on the tool orientation. One reason for the dependency on tool orientation is the varying pitch angle of the individual tooth.

3. Tool deflection control

Based on the estimated tool deflection a P-controller is implemented to compensate for the shape deviation, according to [9, 10]. Subsequently, two different control approaches are discussed. The first approach is the control of the feed override.

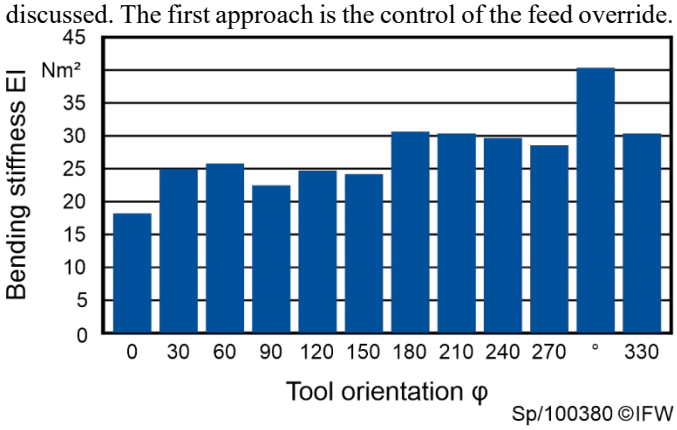

Fig. 4. Bending stiffness estimated by soft collision

Therefore, a set value is specified to define the desired deflection. The controller adapts the override according to the difference between set value and estimated tool deflection error. To avoid zero velocities the override is restricted by a lower boundary of 20% override. Also, an upper boundary of 100% is implemented to limit maximum velocity. As a default, a medium override of 70% is preset. Therefore, it is possible, that feed velocity increases, if the deflection falls below the preset tolerance.

In the second approach, the toolpath is adapted directly according to the tool deflection. Therefore, the controller sets a positional correction orthogonal to the feed direction. Again, lower and upper boundaries are set to avoid positional corrections above 200 µm.

To evaluate both controllers, a workpiece is prepared with a step profile. Subsequently, the steps are removed by straight milling, Fig. 5 a). Consequently, the width of cut increases with every step for 1 mm. Material is removed three times under the same conditions. First, the workpiece is machined without control as a reference (Ref.). Afterward, two more flank milling processes were performed, using the override (Feed) as well as the position control (Pos.). Last, the shape deviation is evaluated by the touch probe, Fig. 5 b) and Fig 5 c).

Fig. 6 shows the reconstructed forces in feed normal direction during positional compensation. The increase in cutting force corresponds to the milled profile. Fig. 6 a) represents the results of the compensation with an unworn tool, while the tool is worn out in Fig. 6 b). For the unworn tool, a shape deviation of less than 5 µm is measured compared to a shape deviation of 50 µm in the reference process without compensation. While the force is higher for the first and the second step of the workpiece, the force decreases when entering the third step. As shown in Fig. 6 b), the process force is lower than the forces during the milling process in Fig. 6a). Contrary to these results, higher forces would have been expected when the tool is worn out. However, the control approach is still capable to reduce the shape deviation by roughly 40 µm which corresponds to a compensation of ~60%. Nevertheless, the remaining error is higher compared to an error of an unworn tool. Since all other parameters are consistent across machining conditions, tool wear seems to have an impact on the whole system.

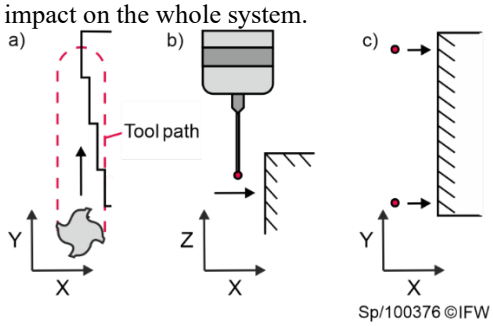

Fig. 5. Setup for the evaluation of the control approach.
a) milling process b) touch probe side view c) touch probe top view

The results of the override control and the position control are shown in Fig. 7. The measurements are restricted to unworn tools. All in all, the drive current based override controller reduces the tool deflection error for about 38%, while the position controller achieves a reduction of 78%. However, the first approach increases the process times significantly: For a width of cut of 3 mm the feed override is reduced to 30%. In contrast, the strain gauge-based solution presented in [10] reaches a reduction of 70% and 80% for both control approaches. A reason for the different performance, comparing the drive current based override control to the sensory spindle slide is the deviation of the real process forces compared to the modeled forces. Nevertheless, it has to be considered that both approaches are implemented on the same machine, but tool and chunk are different.

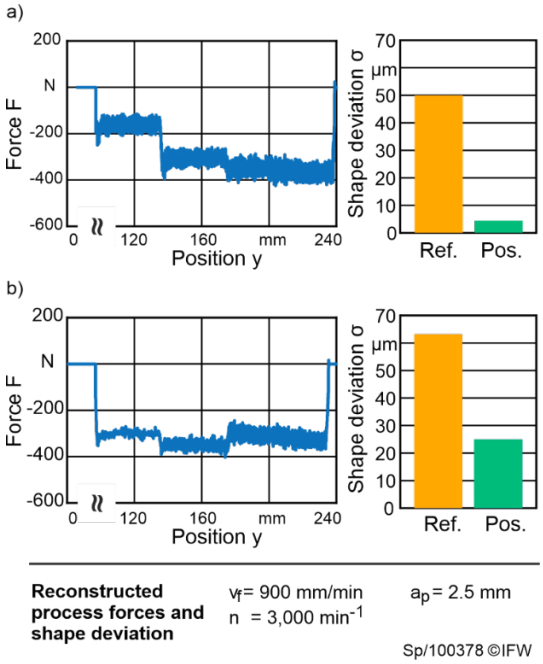

Fig. 6. Process forces in feed normal direction and shape deviation.
a) Unworn tool b) Worn tool

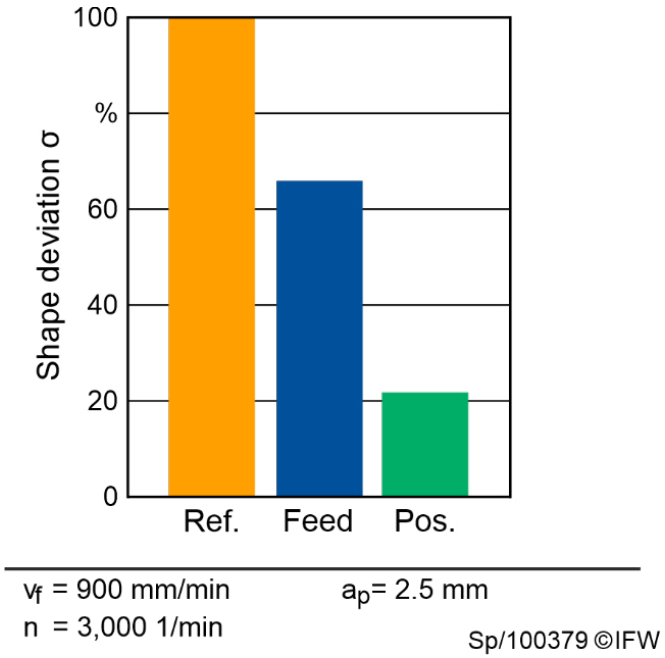

Fig. 7. Tool deflection error depending on the controller

4. Outlook and conclusion

The results show that tool deflection can be compensated by using drive signals. Both approaches, the override control as well as the position controller, significantly reduce the shape deviation of the test workpiece. Especially, the position-based control was able to reduce the shape deviation of the workpiece by 78%. The override control only compensated 38% percent of the tool deflection, but therefore decreases the process forces. It could be shown that the shape deviation can also be reduced for worn tools. Compared to the approach of the sensory slide, which is based on strain gauges, the positional controller achieved similar results. The override controller did not reach the same level of compensation as in [10], where a compensation of 70% to 80% was achieved. A more complex controller and another controller setting may improve the approach. However, the drive signal-based approaches are only compared to the results documented in [10]. For the investigations in [10] the same machine, but other tools and chunks have been used. Therefore, future work will compare both systems by applying the same conditions for each. A more complex controller and another controller setting may improve the drive signal-based compensation. For the control, the quality of the force reconstruction is decisive. Therefore, the force model will be improved by online fusing of the model results with the neural network estimations presented in [15].

Acknowledgments

We thank the DFG for funding this project (grant number DE447/160-1) and our project partner DECKEL MAHO Seebach GmbH.

References

[1] Bogner E, Löwen U, Franke J. Bedeutung der zukünftigen Produktion kundenindividueller Produkte in Losgröße 1. Internationale Perspektiven zur Zukunft der Wertschöpfung. Wiesbaden. Springer Gabler; 63-75; 2018.
[2] Desai KA, Rao PVM. On cutter deflection surface errors in peripheral milling. Journal of Materials Processing Technology 2012;212:2443-2454.
[3] Nghiep TN, Sarhan AAD, Aoyama H. Analysis of tool deflection errors in precision CNC end milling of aerospace Aluminum 6061-T6 alloy. Measurement, 2018;125:476-495.
[4] Rao VS, Rao PVM. Tool deflection compensation in peripheral milling of curved geometries. International Journal of Machine Tools and Manufacture 2006;46:2036-2043.
[5] Dèpincé P, Hascoët JY. Dépincé, Philippe, and Jean-Yves Hascoet. "Active integration of tool deflection effects in end milling. Part 1. Prediction of milled surfaces. International Journal of Machine Tools and Manufacture 2006;46:937-944.
[6] Dèpincé P, Hascoët JY. Active integration of tool deflection effects in end milling. Part 2. Compensation of tool deflection. International Journal of Machine Tools and Manufacture 2006;46:945-956.
[7] Soori M, Arezoo B, Habibi M. Tool deflection error of three-axis computer numerical control milling machines, monitoring and minimizing by a virtual machine. Journal of Manufacturing Science and Engineering 2016;138:2036-2043.
[8] Kim D, Jeon D. Fuzzy-logic control of cutting forces in CNC milling processes using motor currents as indirect force sensors. Precision Engineering 2011;35:143-152.
[9] Denkena B, Dahlmann D, Boujnah H. Tool deflection control by a sensory spindle slide for milling machine tools. Procedia CIRP 2017;62:329-334.
[10] Boujnah H. Kraftsensitiver Spindelschlitten zur online Detektion und Kompensation der Werkzeugabdrängung in der Fräsbearbeitung. Doctoral thesis. Leibniz Universität Hannover: 2019.
[11]Brecher C, Wetzel A, Berners T, Epple A. Increasing Productivity of cutting processes by real-time compensation of tool deflection due to process forces. Journal of Machine Engineering 2019;19:16-27.
[12]Denkena B, Will JC, Möhring B. Tool deflection compensation with an adaptronic milling spindle. International Conference on Smart Machining Systems ICSMS. 2007.
[13]Yang MY, Choi JGA Tool Deflection Compensation System for End Milling Accuracy Improvement. Journal of Manufacturing Science and Engineering 1998;120:222-229.
[14]Zaeh MF, Schnoes F, Obst B, Hartmann D. Combined offline simulation and online adaptation approach for the accuracy improvement of milling robots. CIRP Annals 2020;69:337-340.
[15]Denkena B, Bergmann B, Stoppel D. Reconstruction of process forces in a five-axis milling center with a LSTM neural network in comparison to a model-based approach. Journal of manufacturing and materials processing 2020;4:62-74